Available online at www.sciencedirect.com
ScienceDirect
Journal of Sound and Vibration 307 (2007) 172–186
JOURNAL OF SOUND AND VIBRATION
www.elsevier.com/locate/jsvi

Green's function for a harmonic acoustic point source within seawater overlying a saturated poroelastic seabed

Jian-Fei Lu[a,*], Dong-Sheng Jeng[b]

[a]*Department of Civil Engineering, Jiangsu University, Zhenjiang, Jiangsu 212013, PR China*
[b]*Division of Civil Engineering, Faculty of Engineering, Physical Science, University of Dundee, Dundee DD1 4HN, UK*

Received 1 February 2007; received in revised form 8 June 2007; accepted 30 June 2007

Abstract

In this paper, Green's function for an acoustic source within half-space seawater overlying a porous seabed is established. The half-space seawater is described using the Helmholtz equation, while the seabed is considered as a saturated porous medium and characterized by Biot's theory. Green's function of the half-space seawater has two components: the principal and complementary parts. The principal part of Green's function is the solution for a conventional acoustic point source in an infinite medium, while the complementary part corresponds to the general solution of the Helmholtz equation for the half-space. Green's function of the half-space seabed is obtained by solving Biot's dynamic equations via the Hankel transform method. Using the continuity conditions at the interface between the seawater and the seabed, the closed-form Green's functions for the seawater and the seabed in the frequency–wavenumber domain are determined. The frequency domain Green's function is recovered by the inversion of the Hankel transform. A parametric study is carried out for Green's function in the frequency domain, and a time domain example is presented in terms of frequency domain Green's function. Numerical results show that the permeability of the porous seabed has very little influence on the response of the seawater, while Biot's modulus has a pronounced influence on the wave field.

1. Introduction

Studies of oceanic acoustic waves have numerous applications in areas such as marine exploration, underwater communication, ocean tomography, and ocean telemetry, as acoustic waves are the only kind of waves that can propagate within seawater for a long distance [1]. The ocean environment can usually be treated as an infinite or a half-infinite medium, thus the boundary element method (BEM) is the preferred option for acoustic field simulation. BEM can reduce the dimensions of the domain by one. Due to the adoption of an appropriate Green's function, the radiation condition at infinity is automatically satisfied thus avoiding the artificial boundary layer. As a result, BEM is a very popular method for computational ocean acoustics [2].

*Corresponding author.
E-mail addresses: ljfdoctor@yahoo.com (J.-F. Lu), d.jeng@civil.usyd.edu.au (D.-S. Jeng).

doi:10.1016/j.jsv.2007.06.050

If the computational domain is far from the seabed, the influence of the seabed is negligible and thus the seawater can be treated as an infinite medium. However, for a domain near the seabed, to ensure the accuracy of the acoustic field simulation, the influence of the seabed has to be taken into account. To handle such a problem, a multi-region BEM can be applied [3,4]. The multi-region BEM approach consists of two stages. First, two BEM formulations for the seawater domain and the seabed domain are separately established using the corresponding Green's function. The two formulations are then linked by the continuity condition at the interface between the two domains. It is worth emphasizing that the multi-region BEM will unavoidably entail the discretization of the common boundary for each BEM formulation which will lead to additional computation and discretization errors, particularly for an infinite common boundary. Thus, the BEM formulation which can avoid the discretization of the interface between different domains is desirable.

Many researchers have considered the problem of wave phenomenon in the domain near the interface between seawater and a porous seabed. The reflected and refracted waves due to an incident wave on the interface between the seawater and seabed were discussed by Stoll and Kan [5], Wu et al. [6], and Denneman et al. [7]. Also, a few researchers have investigated the characteristics of surface waves in the vicinity of the interface between a porous medium and a fluid [8–11]. Moreover, a high-frequency limit two-dimensional Green's function for half-space seawater overlying a poroelastic seabed was derived by Feng and Johnson [12], in which the porous medium is assumed to be lossless. However, to date, a three-dimensional Green's function for an acoustic point source located near a half-space poroelastic seabed is still unavailable in the literature.

The aim of this study is to establish Green's function for an acoustic source within half-space seawater overlying a porous seabed. Green's functions for the upper half-space seawater and the poroelastic seabed which contain unknown constants are derived first. The unknown constants of Green's functions are then determined by the continuity condition at the interface. A parametric study is conducted to investigate the influence of permeability and Biot's modulus (M) of poroelasticity on the response of the seawater and the seabed. Also, based on the frequency domain Green's function and inverse Fourier transform method, a time domain example is presented. The derived Green's function will enable the formulation of a BEM, which avoids the discretization of the infinite interface between the seawater and the seabed.

2. Theoretical formulations

In this study, we consider an acoustic source in half-space seawater overlying a porous seabed, as depicted in Fig. 1. The seabed is treated as a half-infinite poroelastic medium and modeled by Biot's poroelastic theory [13–16], while the seawater is described by the conventional Helmholtz equation.

To derive Green's functions, the Fourier transform is involved, which has the following definition [17]:

$$\hat{f}(\omega) := \int_{-\infty}^{+\infty} f(t)\mathrm{e}^{-\mathrm{i}\omega t}\,\mathrm{d}t,\; f(t) := \frac{1}{2\pi}\int_{-\infty}^{+\infty} \hat{f}(\omega)\mathrm{e}^{\mathrm{i}\omega t}\,\mathrm{d}\omega, \tag{1}$$

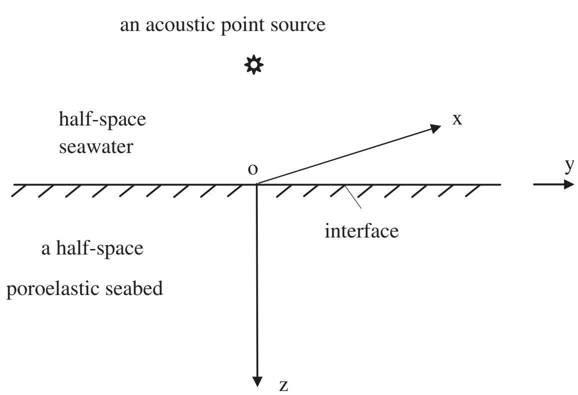

Fig. 1. An acoustic source applied within half-space seawater overlying a saturated half-space porous seabed.

where t and ω denote time and frequency, respectively, and the caret above a variable denotes the Fourier transform.

2.1. Green's function for the half-space seawater

As mentioned previously, the half-space seawater is described by the following Helmholtz equation:

$$\nabla^2 \hat{p}_w + k_w^2 \hat{p}_w = 0, \tag{2}$$

in which $\hat{p}_w$ is the pressure of the seawater, k_w is the wavenumber of the seawater, where $k_w = \omega/v_w$, and ω and v_w are the angular frequency and the acoustic velocity of the seawater, respectively.

Supposing that a harmonic acoustic source is applied at the point $\mathbf{x}_s = (0,0,Z_0) = (0,0,-h)$, then, Green's function for the half-space seawater is determined by the following inhomogeneous Helmholtz equation:

$$\nabla^2 \hat{p}_w + k_w^2 \hat{p}_w = 4\pi\delta(\mathbf{x} - \mathbf{x}_s), \tag{3}$$

where $\delta(\mathbf{x}-\mathbf{x}_s)$ denotes the δ function.

The solution for the above inhomogeneous Helmholtz equation consists of two components: one is homogeneous solution which is determined by Eq. (2), and named as the complementary part (regular part) in this study; the other one is the special solution given by Eq. (3) and named as the principal part (singular part).

Green's function for the principal part has the following form [18]:

$$\hat{p}_{wp} = \frac{1}{R} \mathrm{e}^{-\mathrm{i}k_w R}, \tag{4}$$

where $R = |\mathbf{x}-\mathbf{x}_s|$ and the subscript "p" denotes the principal part.

Since total Green's functions for the seawater and the seabed are axi-symmetrical with respect to the z-axis, to facilitate the implementation of the continuity condition between the seawater and the seabed, Eq. (4) is expanded into the following cylindrical wave [18]:

$$\hat{p}_{wp} = \frac{1}{R} \mathrm{e}^{-\mathrm{i}k_w R} = \int_0^{+\infty} \frac{\mathrm{e}^{-\gamma_w |z+h|}}{\gamma_w} \xi J_0(\xi r)\,\mathrm{d}\xi, \tag{5}$$

where $r = \sqrt{x^2 + y^2}$, ξ is the horizontal wavenumber for the cylindrical wave and $\gamma_w = \sqrt{\xi^2 - k_w^2}$ with $\mathrm{Re}(\gamma_w) \geqslant 0$ and $J_0(*)$ represents zeroth-order first kind Bessel function. Detailed information for Bessel function can be found in Ref. [19]. Also, in view of the time factor $\mathrm{e}^{\mathrm{i}\omega t}$, the imaginary part of γ_w should be non-negative to guarantee vertically propagating waves from the source.

To derive the general solution for the Helmholtz equation in the cylindrical coordinate system (r,θ,z), the Hankel integral transform is involved [17]. The mth-order Hankel transform is defined as follows:

$$\bar{f}^{(m)}(\xi) := \int_0^{+\infty} r f(r) J_m(\xi r) \mathrm{d}r, \tag{6}$$

$$f(r) := \int_0^{+\infty} \xi \bar{f}^{(m)}(\xi) J_m(\xi r) \mathrm{d}\xi, \tag{7}$$

where $J_m(*)$ denotes the mth-order first kind Bessel function and the bar above a variable denotes the Hankel transform.

Complementary part Green's function for the seawater can be obtained by performing the zeroth-order Hankel transform on Eq. (2), which yields

$$\frac{\mathrm{d}^2 \tilde{p}_{wc}^{(0)}}{\mathrm{d}z^2} - (\xi^2 - k_w^2)\tilde{p}_{wc}^{(0)} = \frac{\mathrm{d}^2 \tilde{p}_{wc}^{(0)}}{\mathrm{d}z^2} - \gamma_w^2 \tilde{p}_{wc}^{(0)} = 0, \tag{8}$$

where the tilde above p_{wc} denotes the combination of the Fourier transform and the Hankel transform and the superscript "0" denotes the zeroth-order Hankel transform and the subscript "c" denotes the complementary part Green's function.

The general solution for Eq. (8) can be expressed as

$$\tilde{p}_{wc}^{(0)} = A^{(w)}(\xi,\omega)\mathrm{e}^{\gamma_w z} + B^{(w)}(\xi,\omega)\mathrm{e}^{-\gamma_w z}, \tag{9}$$

To guarantee complementary part Green's function be bounded within the upper half-space, the coefficient $B^{(w)}$ should vanish. Therefore, complementary part Green function's has the form

$$\tilde{p}_{wc}^{(0)} = A^{(w)}(\xi,\omega)\mathrm{e}^{\gamma_w z}. \tag{10}$$

In summary, the pressure and the vertical displacement of Green's function for the seawater have the following form:

$$\tilde{p}_{w}^{(0)} = \tilde{p}_{wp}^{(0)} + \tilde{p}_{wc}^{(0)}, \tag{11}$$

$$\tilde{u}_{wz}^{(0)} = \frac{1}{\rho_w\omega^2}\frac{\partial\tilde{p}_{w}^{(0)}}{\partial z} = \frac{1}{\rho_w\omega^2}\frac{\partial(\tilde{p}_{wp}^{(0)} + \tilde{p}_{wc}^{(0)})}{\partial z}, \tag{12}$$

where ρ_w is the density of the seawater and $\tilde{p}_{wp}^{(0)} = \mathrm{e}^{-\gamma_w|z+h|}/\gamma_w$ (from Eq. (5)).

It is noted that principal part Green's function has a Cauchy-type singularity at the point $\mathbf{x}_s = (0, 0, -h)$, while complementary part Green's function is regular in the upper half-space. Furthermore, the superposition of principal part and complementary part Green's function should fulfill the continuity condition at the interface between the seawater and the seabed.

2.2. *The general expression for Green's function of a poroelastic seabed*

2.2.1. *Biot's theory*

The constitutive equations for a homogeneous porous medium have the form [13–16]

$$\sigma_{ij} = 2\mu\varepsilon_{ij} + \lambda\delta_{ij}e - \alpha\delta_{ij}p, \tag{13}$$

$$p = -\alpha Me + M\zeta, \tag{14}$$

where

$$e = u_{i,i}, \quad \zeta = -w_{i,i}, \tag{15}$$

in which u_i and w_i denote the average solid displacement and the infiltration displacement of the pore fluid; ε_{ij} and e are the strain tensor and the dilatation of the solid skeleton; ζ is the increment of fluid content; σ_{ij} the stress of the bulk porous medium; p the excess pore pressure and δ_{ij} the Kronecker delta. Moreover, λ and μ are Lame constants of the solid skeleton; α and M are Biot parameters [13] accounting for the compressibility of the saturated porous medium.

The equations of motion for the bulk porous medium and the pore fluid are expressed in terms of the displacements u_i and w_i:

$$\mu u_{i,jj} + (\lambda + \alpha^2 M + \mu)u_{j,ji} + \alpha M w_{j,ji} + F_i = \rho_b\ddot{u}_i + \rho_f\ddot{w}_i, \tag{16}$$

$$\alpha M u_{j,ji} + M w_{j,ji} + f_i = \rho_f\ddot{u}_i + m\ddot{w}_i + \frac{\eta}{k}K(t)*\bar{w}_i, \tag{17}$$

where ρ_b and ρ_f denote the density of the porous medium and the density of the pore fluid, and $\rho_b = (1-\phi)\rho_s + \phi\rho_f$, ρ_s is the true density of the solid skeleton and ϕ is the porosity of the porous medium; F_i and f_i are body forces of the porous medium and the pore fluid; $m = a_\infty\rho_f/\phi$ and a_∞ is tortuosity; η and k account for the viscosity of the pore fluid and the permeability of the porous medium, respectively, and $K(t)$ is a time-dependent viscosity correction factor which describes the transition behavior from viscosity-dominated flow in the low-frequency range towards inertia-dominated flow at the high-frequency range [15,20,21]; a superimposed dot on a variable denotes time derivative and the star (*) between two variables denotes time convolution.

Although two independent displacement vectors for the solid skeleton and the pore fluid are used in Biot's theory, there are only four independent variables in the two-phase porous medium [22]. Thus, the displacement of solid skeleton and the pore pressure can be represented by the following potentials [23,24]:

$$\hat{u}_i = \hat{\varphi}_{f,i} + \hat{\varphi}_{s,i} + e_{ijk}\hat{\psi}_{k,j}, \tag{18}$$

$$\hat{p} = A_f\hat{\varphi}_{f,ii} + A_s\hat{\varphi}_{s,ii}, \tag{19}$$

where $\hat{\varphi}_f$ and $\hat{\varphi}_s$ denote scalar potentials corresponding to P_1 wave and P_2 wave, respectively, and $\hat{\psi}_k$ $(k = 1, 2, 3)$ is the vector potential for the porous medium and e_{ijk} is the Levi–Civita symbol, A_f and A_s are two constants. Moreover, in the Cartesian coordinate system, the vector potential $\hat{\psi}_k$ $(k = 1, 2, 3)$ satisfies the following condition:

$$\hat{\psi}_{i,i} = 0. \tag{20.a}$$

The infiltration displacement of the pore fluid can be represented by

$$\hat{w}_i = \frac{\beta_1}{M}[\hat{p}_{,i} - \rho_f\omega^2\hat{u}_i], \tag{20.b}$$

where $\beta_1 = M/[m\omega^2 - \mathrm{i}\omega(\eta/k)\hat{K}(\omega)]$. The potentials $\hat{\varphi}_f$, $\hat{\varphi}_s$ and $\hat{\psi}_k$ $(k = 1, 2, 3)$ satisfy the following Helmholtz equations [23,24]:

$$\nabla^2\hat{\varphi}_f + k_f^2\hat{\varphi}_f = 0, \tag{21}$$

$$\nabla^2\hat{\varphi}_s + k_s^2\hat{\varphi}_s = 0, \tag{22}$$

$$\nabla^2\hat{\psi}_k + k_t^2\hat{\psi}_k = 0, \quad k = 1,\ 2,\ 3, \tag{23}$$

where k_f, k_s and k_t in Eqs. (21)–(23) are the complex wavenumbers for the P_1, P_2, and the S waves of the porous medium and given by [25]

$$k_f^2 = \frac{\beta_2 A_f\omega^2 - \beta_3}{A_f},\ k_s^2 = \frac{\beta_2 A_s\omega^2 - \beta_3}{A_s},\ k_t^2 = \frac{\rho_g\omega^2}{\mu}, \tag{24}$$

where $\beta_2 = 1/(\beta_1\omega^2)$, $\beta_3 = \rho_f\omega^2 - \alpha[m\omega^2 - \mathrm{i}\omega(\eta/k)\hat{K}(\omega)]$, $\beta_4 = \rho_f\omega^2\beta_1/M$, $\rho_g = \rho_b - \beta_4\rho_f$, and $\hat{K}(\omega)$ denotes the Fourier transform of $K(t)$ in Eq. (17), and two constants A_f and A_s are given by [25]

$$A_{f,s}^2 + \frac{[\rho_g\omega^2 - \alpha_g\beta_3 - (\lambda + 2\mu)\beta_2\omega^2]}{\alpha_g\beta_2\omega^2}A_{f,s} + \frac{(\lambda + 2\mu)\beta_3}{\alpha_g\beta_2\omega^2} = 0, \tag{25}$$

in which $\alpha_g = \alpha - \beta_4$.

2.2.2. Derivation of the general expression for Green's function of the seabed

As stated previously, Green's function of the seabed is axi-symmetrical with respect to the z-axis (Fig. 1). In this case, the vector potential $\hat{\psi}_k$ $(k = 1, 2, 3)$ can be represented by just one scalar potential $\hat{\eta}$ in the cylindrical coordinate system [26]. Thus, in the cylindrical coordinate system, the Helmholtz Eqs. (21)–(23) can be re-written as

$$\left(\frac{\partial^2}{\partial r^2} + \frac{1}{r}\frac{\partial}{\partial r} + \frac{\partial^2}{\partial z^2}\right)\hat{\varphi}_f + k_f^2\hat{\varphi}_f = 0, \tag{26}$$

$$\left(\frac{\partial^2}{\partial r^2} + \frac{1}{r}\frac{\partial}{\partial r} + \frac{\partial^2}{\partial z^2}\right)\hat{\varphi}_s + k_s^2\hat{\varphi}_s = 0 \tag{27}$$

$$\left(\frac{\partial^2}{\partial r^2} + \frac{1}{r}\frac{\partial}{\partial r} + \frac{\partial^2}{\partial z^2}\right)\hat{\eta} + k_t^2\hat{\eta} = 0. \tag{28}$$

The displacements of the solid frame and the pore fluid can be expressed in terms of the potentials in the cylindrical coordinate system (r, θ, z) as follows:

$$\hat{u}_r = \frac{\partial \hat{\varphi}_f}{\partial r} + \frac{\partial \hat{\varphi}_s}{\partial r} + \frac{\partial^2 \hat{\eta}}{\partial r \partial z}, \tag{29}$$

$$\hat{u}_z = \frac{\partial \hat{\varphi}_f}{\partial z} + \frac{\partial \hat{\varphi}_s}{\partial z} - \frac{1}{r}\frac{\partial}{\partial r}\left(r\frac{\partial \hat{\eta}}{\partial r}\right), \tag{30}$$

$$\hat{w}_r = \frac{M}{\beta_1}\frac{\partial \hat{p}}{\partial r} - \frac{M\rho_f\omega^2}{\beta_1}\hat{u}_r, \tag{31}$$

$$\hat{w}_z = \frac{M}{\beta_1}\frac{\partial \hat{p}}{\partial z} - \frac{M\rho_f\omega^2}{\beta_1}\hat{u}_z. \tag{32}$$

Performing the zeroth-order Hankel transform with respect to radial coordinate r on Eqs. (26)–(28), the general solutions of the potentials, $\tilde{\varphi}_f$, $\tilde{\varphi}_s$, and $\tilde{\eta}$ in the frequency–wavenumber domain are obtained as follows:

$$\tilde{\varphi}_f^{(0)}(\xi, z, \omega) = A^{(s)}(\xi, \omega)\mathrm{e}^{\gamma_f z} + B^{(s)}(\xi, \omega)\mathrm{e}^{-\gamma_f z}, \tag{33}$$

$$\tilde{\varphi}_s^{(0)}(\xi, z, \omega) = C^{(s)}(\xi, \omega)\mathrm{e}^{\gamma_s z} + D^{(s)}(\xi, \omega)\mathrm{e}^{-\gamma_s z}, \tag{34}$$

$$\tilde{\eta}^{(0)}(\xi, z, \omega) = E^{(s)}(\xi, \omega)\mathrm{e}^{\gamma_t z} + F^{(s)}(\xi, \omega)\mathrm{e}^{-\gamma_t z}, \tag{35}$$

where the superscript 0 denotes the zeroth-order Hankel transform and $A^{(s)}(\xi, \omega)$, $B^{(s)}(\xi, \omega)$, $C^{(s)}(\xi, \omega)$, $D^{(s)}(\xi, \omega)$, $E^{(s)}(\xi, \omega)$, $F^{(s)}(\xi, \omega)$ are arbitrary constants. In Eqs. (33)–(35), γ_f, γ_s, and γ_t are the quantities related to the vertical wavenumbers for the P_1, P_2, and S wave of the porous medium and are given by

$$\gamma_f = \sqrt{\xi^2 - k_f^2}, \quad \gamma_s = \sqrt{\xi^2 - k_s^2}, \quad \gamma_t = \sqrt{\xi^2 - k_t^2}. \tag{36}$$

Note that the real part of $\gamma_k,\ k = f, s, t$ in Eq. (36) should be always non-negative to guarantee the bounded condition at infinity.

By using the Hankel transform method, the displacements, the stresses, and the pore pressure can also be represented by the potentials

$$\tilde{u}_r^{(1)} = -\xi\tilde{\varphi}_f^{(0)} - \xi\tilde{\varphi}_s^{(0)} - \xi\frac{\mathrm{d}\tilde{\eta}^{(0)}}{\mathrm{d}z}, \tag{37}$$

$$\tilde{u}_z^{(0)} = \frac{\mathrm{d}\tilde{\varphi}_s^{(0)}}{\mathrm{d}z} + \frac{\mathrm{d}\tilde{\varphi}_f^{(0)}}{\mathrm{d}z} + \xi^2\tilde{\eta}^{(0)}, \tag{38}$$

$$\tilde{w}_r^{(1)} = -\frac{\xi}{\beta_1}\tilde{p}^{(0)} - \frac{\rho_f\omega^2}{\beta_1}\tilde{u}_r^{(1)}, \tag{39}$$

$$\tilde{w}_z^{(0)} = \frac{1}{\beta_1}\frac{\partial \tilde{p}^{(0)}}{\partial z} - \frac{\rho_f\omega^2}{\beta_1}\tilde{u}_z^{(0)}, \tag{40}$$

$$\tilde{p}^{(0)} = -A_f k_f^2\tilde{\varphi}_f^{(0)} - A_s k_s^2\tilde{\varphi}_s^{(0)}, \tag{41}$$

$$\tilde{\sigma}_{zr}^{(1)} = \mu\frac{\mathrm{d}\tilde{u}_r^{(1)}}{\mathrm{d}z} - \mu\xi\tilde{u}_z^{(0)}, \tag{42}$$

$$\tilde{\sigma}_{zz}^{(0)} = 2\mu \frac{d\tilde{u}_z^{(0)}}{dz} + \lambda \left[\left(\frac{d^2\tilde{\varphi}_f^{(0)}}{dz^2} - \xi^2 \tilde{\varphi}_f^{(0)} \right) + \left(\frac{d^2\tilde{\varphi}_s^{(0)}}{dz^2} - \xi^2 \tilde{\varphi}_s^{(0)} \right) \right] - \alpha \tilde{p}^{(0)}. \tag{43}$$

To guarantee Green's function of the seabed to be bounded in the lower half-space, constants $A^{(s)}(\xi, \omega)$, $C^{(s)}(\xi, \omega)$, and $E^{(s)}(\xi, \omega)$ in Eqs. (33)–(35) should vanish. Thus, the potentials for Green's function of the seabed have the form

$$\tilde{\varphi}_f^{(0)}(\xi, z, \omega) = B^{(s)}(\xi, \omega) e^{-\gamma_f z}, \tag{44}$$

$$\tilde{\varphi}_s^{(0)}(\xi, z, \omega) = D^{(s)}(\xi, \omega) e^{-\gamma_s z}, \tag{45}$$

$$\tilde{\eta}^{(0)}(\xi, z, \omega) = F^{(s)}(\xi, \omega) e^{-\gamma_t z}. \tag{46}$$

Substitution of Eqs. (44)–(46) into Eqs. (37)–(43), the displacements, the stresses, and the pore pressure for Green's function of the seabed can be determined. Note that Green's function of the seabed still contains three unknown arbitrary constants, which will be determined by the continuity condition at the interface.

2.3. Determination of Green's functions by the continuity condition at the interface

In this section, the continuity condition at the interface between the seawater and the seabed will be used to determine the constants involved in Green's functions for the seawater and the seabed. The continuity condition at the interface can be divided into two kinds: the first kind corresponds to a permeable seabed surface, while the second kind is associated with an impermeable seabed surface.

2.3.1. A permeable seabed surface

For a permeable seabed surface, the continuity condition in the frequency–wavenumber domain has the following form [5]:

$$\tilde{u}_{wz}^{(0)} = \tilde{u}_z^{(0)} + \tilde{w}_z^{(0)},\ \tilde{p}_w^{(0)} = -\tilde{\sigma}_{zz}^{(0)},\ \tilde{\sigma}_{zr}^{(1)} = 0,\ \tilde{p}_w^{(0)} = \tilde{p}^{(0)}. \tag{47}$$

Substituting Eqs. (11)–(12), (37)–(43), and (44)–(46) into Eq. (47), the constants $B^{(s)}(\xi, \omega)$, $D^{(s)}(\xi, \omega)$, $F^{(s)}(\xi, \omega)$, and $A^{(w)}(\xi, \omega)$ for the permeable seabed surface have the following expressions:

$$B^{(s)}(\xi, \omega) = 2e^{z_o\gamma_w} \beta_1 \gamma_f (k_s^2(\gamma_t^2 + \xi^2)(A_s(\alpha - 1) - \lambda) + 2\mu\gamma_s(\gamma_s\gamma_t^2 + (\gamma_s - 2\gamma_t)\xi^2))/\Pi_{p1}, \tag{48}$$

$$D^{(s)}(\xi, \omega) = 2e^{z_o\gamma_w} \beta_1 \gamma_f (4\mu\gamma_f\gamma_t\xi^2 - (k_f^2(A_f(\alpha - 1) - \lambda) + 2\mu\gamma_f^2)(\gamma_t^2 + \xi^2))/\Pi_{p1}, \tag{49}$$

$$F^{(s)}(\xi, \omega) = -4e^{z_o\gamma_w} \beta_1 \gamma_f (k_s^2 A_s \gamma_f (1 - \alpha) - k_f^2 \gamma_s (A_f(1 - \alpha) + \lambda) + \lambda k_s^2 \gamma_f + 2\mu\gamma_f\gamma_s(\gamma_f - \gamma_s))/\Pi_{p1}, \tag{50}$$

$$A^{(w)}(\xi, \omega) = \Gamma_{Aw}/\Pi_{p2}, \tag{51}$$

$$\begin{aligned}
\Pi_{p1} = {} & (-A_s k_s^2 \gamma_f (\alpha - 1) + k_f^2 \gamma_s (A_f(\alpha - 1) - \lambda) + k_s^2 \gamma_f \lambda + 2\mu\gamma_f\gamma_s(\gamma_f - \gamma_s)) \\
& \times (\gamma_f \rho_w \omega^2 (\gamma_t^2 - \xi^2)(\rho_f \omega^2 - \beta_1) + A_f k_f^2 (\gamma_t^2 + \xi^2)(\beta_1 \gamma_w + \gamma_f \rho_w \omega^2)) \\
& + (k_f^2 (\gamma_t^2 + \xi^2)(\lambda + A_f(1 - \alpha)) - 2\mu\gamma_f(\gamma_f\gamma_t^2 + \xi^2(\gamma_f - 2\gamma_t))) \\
& \times (A_f k_f^2 \gamma_s (\beta_1 \gamma_w + \gamma_f \rho_w \omega^2) - A_s k_s^2 \gamma_f (\beta_1 \gamma_w + \gamma_s \rho_w \omega^2)),
\end{aligned} \tag{52}$$

$$\begin{aligned}\Gamma_{Aw} = &(\mathrm{e}^{z_0\gamma_w} + A_f B^{(s)}\gamma_w k_f^2)(\lambda k_s^2(\gamma_t^2+\xi^2) - 2\mu\gamma_s(\gamma_s\gamma_t^2 + (\gamma_s - 2\gamma_t)\xi^2)) \\ &- A_s k_s^2(\mathrm{e}^{z_0\gamma_w}(\alpha-1)(\gamma_t^2+\xi^2) + B^{(s)}\gamma_w(\lambda k_f^2(\gamma_t^2+\xi^2) \\ &- 2\mu\gamma_f(\gamma_f\gamma_t^2 + (\gamma_f - 2\gamma_t)\xi^2))),\end{aligned} \tag{53}$$

$$\Pi_{p2} = \gamma_w(k_s^2(\gamma_t^2+\xi^2)(A_s(\alpha-1)-\lambda) + 2\mu\gamma_s(\gamma_s\gamma_t^2 + (\gamma_s - 2\gamma_t)\xi^2)). \tag{54}$$

2.3.2. An impermeable seabed surface

For an impermeable seabed surface, the continuity condition in the frequency–wavenumber domain has the following form [5]:

$$\tilde{u}_{wz}^{(0)} = \tilde{u}_z^{(0)},\ \tilde{w}_z^{(0)} = 0,\ \tilde{p}_w^{(0)} = -\tilde{\sigma}_{zz}^{(0)},\ \tilde{\sigma}_{zr}^{(1)} = 0. \tag{55}$$

Likewise, substituting Eqs. (11)–(12), (37)–(43) and (44)–(46) into Eq. (55), the constants $B^{(s)}(\xi,\ \omega)$, $D^{(s)}(\xi,\ \omega)$, $F^{(s)}(\xi,\ \omega)$, and $A^{(w)}(\xi,\ \omega)$ for the impermeable seabed surface have the following expressions:

$$B^{(s)}(\xi,\ \omega) = 2\mathrm{e}^{z_o\gamma_w}\gamma_s(A_s k_s^2(\gamma_t^2+\xi^2) + \rho_f\omega^2(\gamma_t^2-\xi^2))/\Pi_{ip1}, \tag{56}$$

$$D^{(s)}(\xi,\ \omega) = -2\mathrm{e}^{z_o\gamma_w}\gamma_f(A_f k_f^2(\gamma_t^2+\xi^2) + \rho_f\omega^2(\gamma_t^2-\xi^2))/\Pi_{ip1}, \tag{57}$$

$$F^{(s)}(\xi,\ \omega) = -4\mathrm{e}^{z_o\gamma_w}\gamma_f\gamma_s(k_f^2A_f - k_s^2A_s)/\Pi_{ip1}, \tag{58}$$

$$\begin{aligned}A^{(w)}(\xi,\ \omega) = &-\alpha A_f k_f^2 B^{(s)} - \frac{\mathrm{e}^{z_o\gamma_w}}{\gamma_w} + \lambda k_f^2 B^{(s)} - 2\mu\gamma_f^2 B^{(s)} - 4\mu\xi^2\gamma_f\gamma_s\gamma_t(A_f k_f^2 - A_s k_s^2)B^{(s)}/\Pi_{ip2} \\ &+ \gamma_f B^{(s)}(k_s^2(\alpha A_s - \lambda) + 2\mu\gamma_s^2)(A_f k_f^2(\gamma_t^2+\xi^2) + \rho_f\omega^2(\gamma_t^2-\xi^2))/\Pi_{ip2},\end{aligned} \tag{59}$$

$$\begin{aligned}\Pi_{ip1} = &A_s k_s^2\gamma_s\gamma_w(k_f^2\lambda(\gamma_t^2+\xi^2) - 2\mu\gamma_f(\gamma_f\gamma_t^2 + (\gamma_f - 2\gamma_t)\xi^2)) + A_f k_f^2\gamma_w(k_s^2(\gamma_t^2+\xi^2)(A_s\alpha(\gamma_f-\gamma_s) - \lambda\gamma_f) \\ &+ 2\mu\gamma_f\gamma_s(\gamma_s\gamma_t^2 + (\gamma_s - 2\gamma_t)\xi^2)) + (\gamma_t^2 - \xi^2)(-\gamma_w(k_f^2\gamma_s(\alpha A_f - \lambda) + k_s^2\gamma_f\lambda \\ &+ 2\mu\gamma_f\gamma_s(\gamma_f - \gamma_s))\rho_f + A_f k_f^2\gamma_f\gamma_s\rho_w + A_s k_s^2\gamma_f(\alpha\gamma_w\rho_f + \gamma_s\rho_w))\omega^2,\end{aligned} \tag{60}$$

$$\Pi_{ip2} = A_s k_s^2\gamma_s(\gamma_t^2+\xi^2) + \gamma_s\rho_f\omega^2(\gamma_t^2-\xi^2). \tag{61}$$

Once the constants, $B^{(s)}(\xi,\ \omega)$, $D^{(s)}(\xi,\ \omega)$, $F^{(s)}(\xi,\ \omega)$, and $A^{(w)}(\xi,\ \omega)$ are determined, the displacements, the stresses, and the pore pressure of the seabed in the frequency–wavenumber domain can be evaluated by Eqs. (37)–(43) and (44)–(46). The displacements, the stresses, and the pore pressure in the frequency domain can be obtained by inversion of the Hankel transform, which can be represented uniformly by the following expression:

$$\hat{\Omega}(\mathbf{x},\omega) = \int_0^{+\infty}[\tilde{\Omega}(\xi,z,\omega)]\xi J_m(\xi r)d\xi, \tag{62}$$

where $\hat{\Omega}(\mathbf{x},\omega)$ and $\tilde{\Omega}(\xi,z,\omega)$ denote the displacements, the stresses, and the pore pressure in the frequency and frequency–wavenumber domain, and m (zero or one) is the corresponding order of the Hankel transform. Note that as closed-form frequency domain Green's function for the seabed can not be obtained by the inversion of the Hankel transform via (62), thus, only numerical Green's function can be evaluated using the fast fourier transform (FFT) algorithm [27,28] or a direct integration of integral (62).

The pressure of the seawater in the frequency domain has the following form:

$$\hat{p}_w(\mathbf{x},\omega) = \frac{1}{R}\mathrm{e}^{-\mathrm{i}k_wR} + \int_0^{+\infty}[A^{(w)}(\xi,\omega)\mathrm{e}^{\gamma_w z}]\xi J_0(\xi r)\mathrm{d}\xi. \tag{63}$$

Note that the implementation of BEM requires the treatment of singular part Green's function separately. Thus, Eq. (63), which has a separate singular part and regular part Green's function, will facilitate the implementation of BEM for the seawater significantly.

3. Numerical results

3.1. Influence of the permeability on the response of the seawater and the seabed

In this example, the influence of the permeability of the seabed on the response of the seawater and the seabed will be examined. The pressure of the seawater ($\hat{p}_w$), the pore pressure ($\hat{p}$), and the stress ($\hat{\sigma}_{zz}$) of the seabed will be calculated. The surface of the seabed is assumed to be permeable. Parameters for the porous medium are assumed the following values: $\mu = 2.0 \times 10^7\,\text{Pa}$, $\lambda = 2.0 \times 10^7\,\text{Pa}$, $\rho_s = 2.3 \times 10^3\,\text{kg/m}^3$, $\rho_f = 1.0 \times 10^3\,\text{kg/m}^3$, $a_\infty = 3$, $\alpha = 0.9$, $M = 3.0 \times 10^9\,\text{Pa}$, $\phi = 0.3$, $\eta = 10. \times 10^{-3}\,\text{Pa s}$, $k = 1.0 \times 10^{-10}$, 1.0×10^{-11}, $1.0 \times 10^{-12}\,\text{m}^2$, respectively. Parameters for the seawater are as follows: $\rho_w = 1.0 \times 10^3\,\text{kg/m}^3$ and velocity $v_w = 1414.0\,\text{m/s}$.

For acoustic waves which are beyond the low-frequency range of Biot's theory [14], Biot's theory for high-frequency waves should be applied [15]. To describe the high-frequency viscous interaction between the solid skeleton and the pore fluid, the JKD model [20], which can treat lower frequency and higher frequency fluid–solid interaction uniformly, is incorporated with Biot's theory [15]. According to Johnson et al. [20], the frequency domain viscosity correction function corresponding to the time domain $K(t)$ in Eq. (17) assumes the form

$$\hat{K}(\omega) = \left(1 + \mathrm{i}\frac{\omega}{\omega_c}\chi_g\right)^{1/2}, \quad \omega_c = \frac{\eta\phi}{\rho_f a_\infty k}, \tag{64}$$

where ω_c is the transition frequency [20,21], which characterizes the transition from the viscosity dominated flow in the low-frequency range towards the inertia-dominated flow at the high-frequency range, and χ_g is the pore geometry term which is equal to $\frac{1}{2}$ for most porous media [21].

The acoustic source is located at $(r, z) = (0.0m, -1.0m)$ and the frequency ω of the source takes the values $0–10^5\,1/\text{s}$. Four observation points in the seawater and the seabed are located at $(r, z) = (1.0\,m, -0.5\,m)$, $(1.0\,m, 0.5\,m)$ and $(r, z) = (15.0\,m, -0.5\,m)$, and $(15.0\,m,\ 0.5\,m)$, respectively. The pressure of the seawater ($\hat{p}_w$), the pore pressure ($\hat{p}$), and the stress ($\hat{\sigma}_{zz}$) of the seabed versus the frequency for the three cases of $k = 1.0 \times 10^{-10}$, 1.0×10^{-11}, and $1.0 \times 10^{-12}\,\text{m}^2$ at the points with $r = 1\,\text{m}$ are plotted in Fig. 2(a)–(c), respectively, while those for the points with $r = 15\,\text{m}$ are plotted in Fig. 2(d)–(f). Also, the pressure of the seawater with the fixed boundary condition (vertical displacement vanishes at the interface) at the interface ($z = 0$) is illustrated in Fig. 2(a) and (d).

Fig. 2(a) shows that the permeability of the seabed has very little influence on the pressure of the seawater. Also, the pressures of the seawater for the three cases are smaller than that for the fixed boundary case. Fig. 2(b) and (c) indicate that at lower frequency range, the difference between the responses of the seabed for the three cases is not very large. However, with increasing frequency, the differences between the responses of the seabed for the three cases become significant. Fig. 2(d) illustrates the pressure of the seawater at the point $(r, z) = (15.0\,m, -0.5\,m)$: compared with the pressure at the point $(r, z) = (1.0\,m, -0.5\,m)$, it decreases considerably; also, the pressure of the seawater at this point is less oscillatory than that at the point $(r, z) = (1.0\,m, -0.5\,m)$; moreover, it is not always smaller than the pressure of the seawater with the fixed boundary. Fig. 2(e) and (f) show that the variation of the response of the porous seabed in the low-frequency range becomes less steeper when the radial distance varies from $r = 1$ to $15\,\text{m}$.

3.2. Influence of modulus M on the response of the seawater and the seabed

In this example, the influence of Biot's modulus M of the seabed on the response of the seabed and the seawater will be investigated. The pressure of the seawater $\hat{p}_w$, the pore pressure $\hat{p}$, the stress $\hat{\sigma}_{zz}$, and the displacement $\hat{u}_z$ of the seabed are calculated. The surface of the seabed is assumed to be impermeable. Parameters for the porous medium are assumed as the following values: $\mu = 2.0 \times 10^7\,\text{Pa}$, $\lambda = 2.0 \times 10^7\,\text{Pa}$, $\rho_s = 2.3\,10^3\,\text{kg/m}^3$, $\rho_f = 1.0 \times 10^3\,\text{kg/m}^3$, $a_\infty = 3$, $\alpha = 0.9$, $M = 2.0 \times 10^8$, 1.0×10^9, $5.0 \times 10^9\,\text{Pa}$, $\phi = 0.3$,

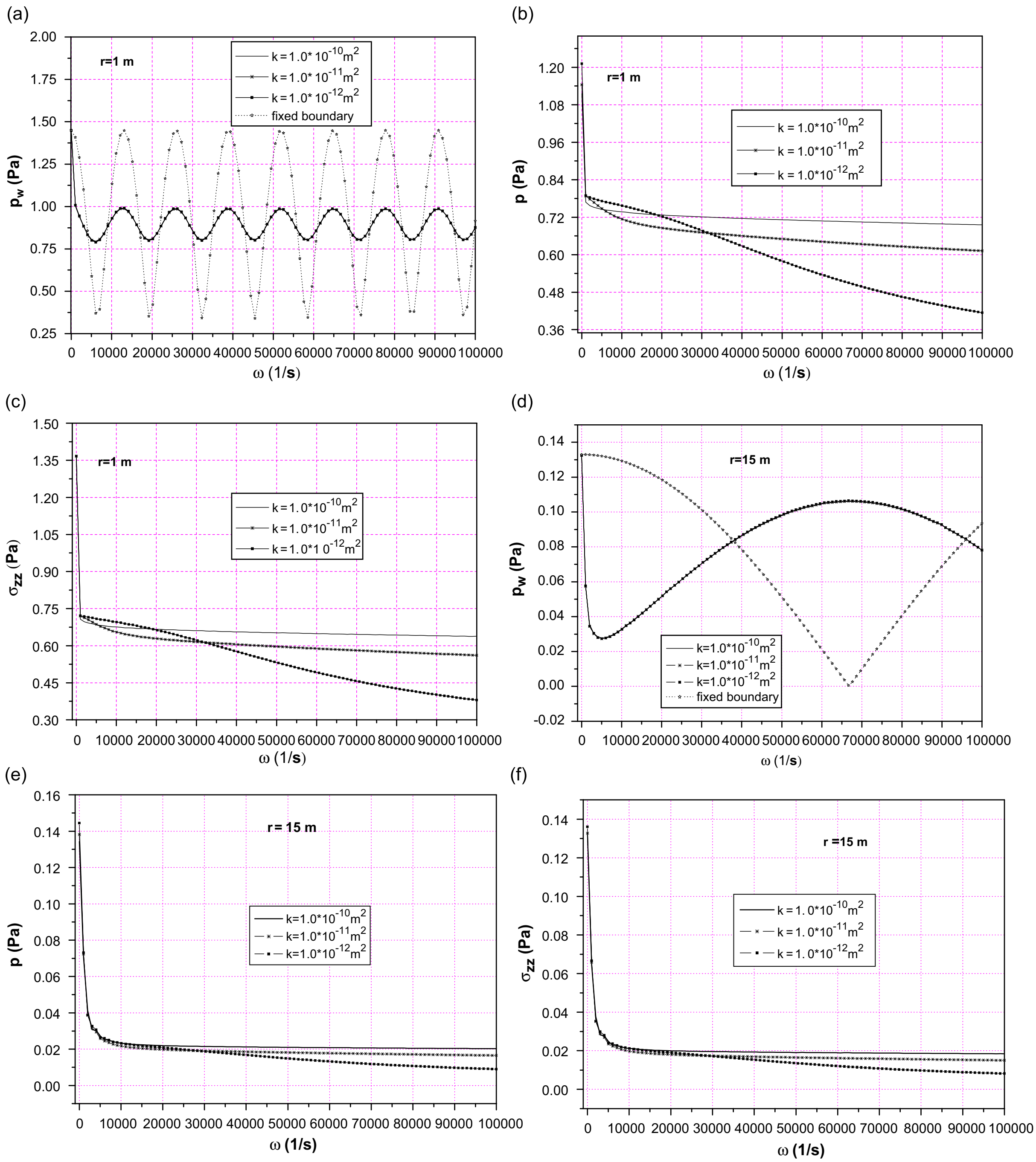

Fig. 2. The response of the seawater and the seabed to an acoustic source located at $(r, z) = (0.0\,m, -1.0\,m)$with angular frequency $\omega = 0{-}10^5\,1/\mathrm{s}$. Three cases corresponding to the permeability of the seabed $k = 1.0 \times 10^{-10}$, 1.0×10^{-11}, and $1.0 \times 10^{-12}\,\mathrm{m}^2$, respectively, are calculated: (a) variation of the pressure of the seawater $\hat{p}_w$ at the point $(r, z) = (1.0m, -0.5m)$ versus angular frequency ($\omega = 0{-}10^5\,1/\mathrm{s}$); (b) variation of the pressure $\hat{p}$ of the seabed at the point $(r, z) = (1.0\,m, 0.5\,m)$ versus angular frequency ($\omega = 0{-}10^5\,1/\mathrm{s}$); (c) variation of the stress $\hat{\sigma}_{zz}$of the seabed at the point $(r, z) = (1.0m, 0.5m)$ versus angular frequency ($\omega = 0{-}10^5\,1/\mathrm{s}$); (d) variation of the pressure of the seawater $\hat{p}_w$ at the point $(r, z) = (15.0\,m, -0.5\,m)$ versus angular frequency ($\omega = 0{-}10^5\,1/\mathrm{s}$); (e) variation of the pressure $\hat{p}$ of the seabed at the point $(r, z) = (15.0\,m, 0.5\,m)$ versus angular frequency ($\omega = 0{-}10^5\,1/\mathrm{s}$); (f) variation of the stress $\hat{\sigma}_{zz}$ of the seabed at the point $(r, z) = (15.0\,m, 0.5\,m)$ versus angular frequency ($\omega = 0{-}10^5\,1/\mathrm{s}$).

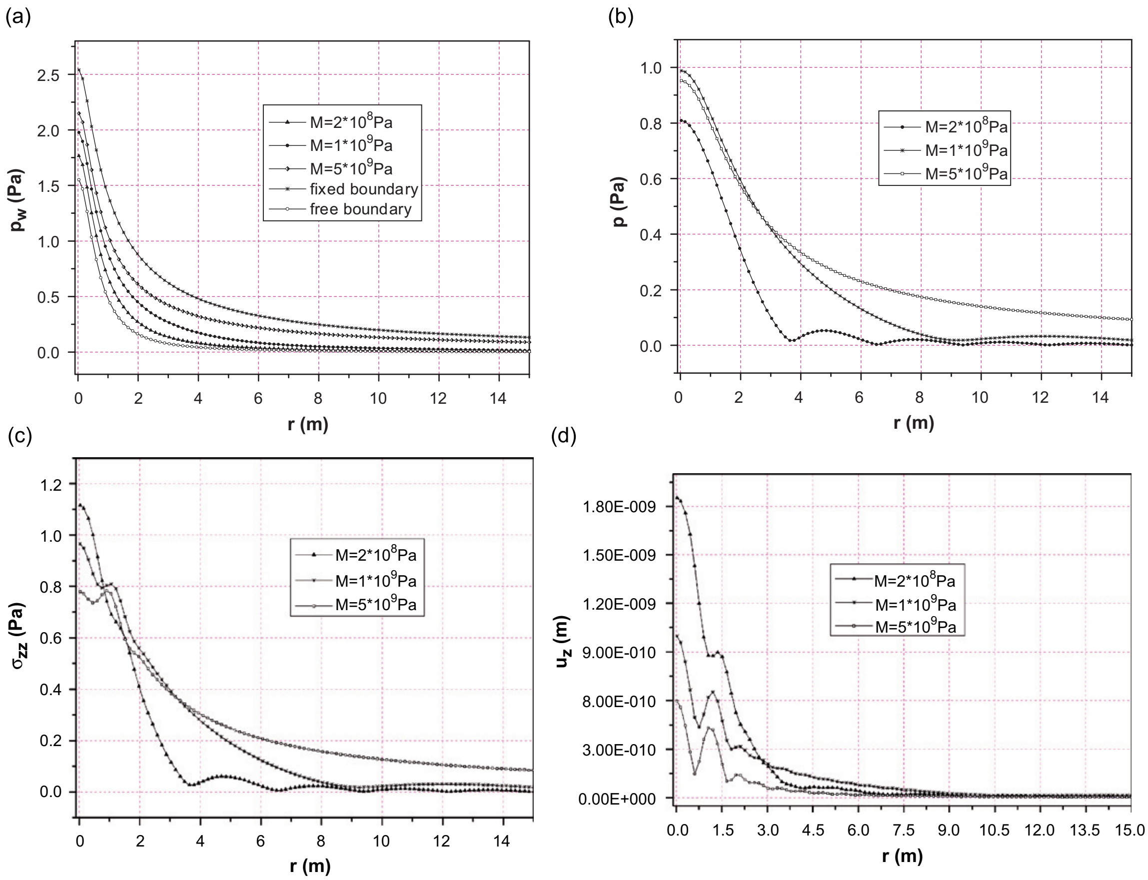

Fig. 3. The response of the seawater and the seabed to an acoustic source located at $(r,z) = (0.0\,m, -0.5\,m)$with angular frequency $\omega = 10^3$ 1/s. Three cases corresponding to Biot's modulus of the seabed $M = 2.0\times10^8$, 1.0×10^9, 5.0×10^9 Pa, respectively, are calculated: (a) the pressure $\hat{p}_w$ of the seawater at points $(r,z) = (0.0-15m, -1.0m)$; (b) the pore pressure $\hat{p}$ of the seabed at points $(r,z) = (0.0-15\,m, 1.0\,m)$; (c) the stress $\hat{\sigma}_{zz}$ of the seabed at points $(r,z) = (0.0-15\,m, -1.0\,m)$; (d) the displacement $\hat{u}_z$ of the seabed at points $(r,z) = (0.0-15\,m, -1.0\,m)$.

$\eta = 1.0\times10^{-3}$ Pa s, $k = 1.0\times10^{-12}\,\mathrm{m}^2$. The parameters for the seawater are as follows: $\rho_w = 1.0\times10^3\,\mathrm{kg/m}^3$ and velocity $v_w = 1414.0\,\mathrm{m/s}$.

The acoustic source is located at $(r,z) = (0.0\,m, -0.5\,m)$ and the frequency ω of the source is equal to 10^3 1/s. Observation points in the seawater and the seabed are located at $(r,z) = (0.0\sim15\,m, -1.0\,m)$ and $(r,z) = (0.0\sim15m, 1.0m)$. The pressure of the seawater $\hat{p}_w$, the pore pressure $\hat{p}$, the stress $\hat{\sigma}_{zz}$, and the displacement $\hat{u}_z$ for the three cases with $M = 2.0\times10^8$, 1.0×10^9, and 5.0×10^9 Pa are plotted in Fig. 3(a)–(d), respectively. Also, the pressures for the seawater with a fixed boundary and a free boundary (with vanishing pressure) at the interface ($z = 0$) are plotted in Fig. 3(a).

Fig. 3(a) shows that the modulus M of the seabed has a considerable influence on the pressure of the seawater: with increasing modulus M, the pressure of the seawater increases. Since modulus M is associated with the compressibility of the pore fluid it is possible to distinguish different pore fluids according to the reflected wave from the porous seabed. Also, it is interesting to notice that with increasing modulus M, the seawater pressure curves shift from the free boundary curve to the fixed boundary curve gradually. The pore pressure ($\hat{p}$) and the stress ($\hat{\sigma}_{zz}$) for points with large coordinate r increase with increasing modulus M. However, for a smaller coordinate r, the stress $\hat{\sigma}_{zz}$ decreases with increasing modulus M. Fig. 3(d) shows that for a small r, the vertical displacement $\hat{u}_z$ decreases with increasing modulus M. Also, it decreases very quickly with increasing coordinate r.

3.3. The time domain response of the seawater and seabed due to an acoustic point source located in the seawater

In this example, based on the frequency domain Green's function, the time domain response of the seawater and the seabed due to an acoustic point source located in the seawater is calculated using inverse Fourier transform method, which is implemented by the FFT method. Parameters for the porous medium are assumed as the following values: $\mu = 5.0 \times 10^9\,\mathrm{Pa}$, $\lambda = 10.0 \times 10^9\,\mathrm{Pa}$, $\rho_s = 2.5 \times 10^3\,\mathrm{kg/m^3}$, $\rho_f = 1.0 \times 10^3\,\mathrm{kg/m^3}$, $a_\infty = 3$, $\alpha = 0.7$, $M = 10.0 \times 10^9\,\mathrm{Pa}$, $\phi = 0.33$, $\eta = 1.0 \times 10^{-3}\,\mathrm{Pa\,s}$, $k = 1.0 \times 10^{-8}$, and $1.0 \times 10^{-12}\,\mathrm{m^2}$. Parameters for the seawater are as follows: $\rho_w = 1.0 \times 10^3\,\mathrm{kg/m^3}$ and velocity $v_w = 1414.0\,\mathrm{m/s}$.

The acoustic point source is of the Ricker wavelet function [29] given by

$$R(t) = \left[\frac{\omega_c^2(t-t_s)^2}{2} - 1\right] \mathrm{e}^{-\omega_c^2(t-t_s)^2/4}, \tag{65}$$

in which the central frequency f_c and the time shift t_s of the acoustic point source are $f_c = 1 \times 10^3\,\mathrm{Hz}$, and $t_s = 2.5 \times 10^{-3}\,\mathrm{s}$ with $f_c = \omega_c/(2\pi)$. The acoustic source is located at $(r, z) = (0.0\,m, -10.0\,m)$. Observation points in the seawater and the seabed are located at $(r, z) = (20.0\,m, -20.0\,m)$ and $(r, z) = (20.0\,m, 20.0\,m)$. The pressure of the seawater p_w, the pore pressure p, the stress σ_{zz} and the displacement u_z of the seabed with a permeable and an impermeable surface for permeability $k = 1.0 \times 10^{-8}$, $1.0 \times 10^{-12}\,\mathrm{m^2}$ are plotted in Figs. 4 and 5, respectively. When retrieving the time domain response from frequency domain Green's function via

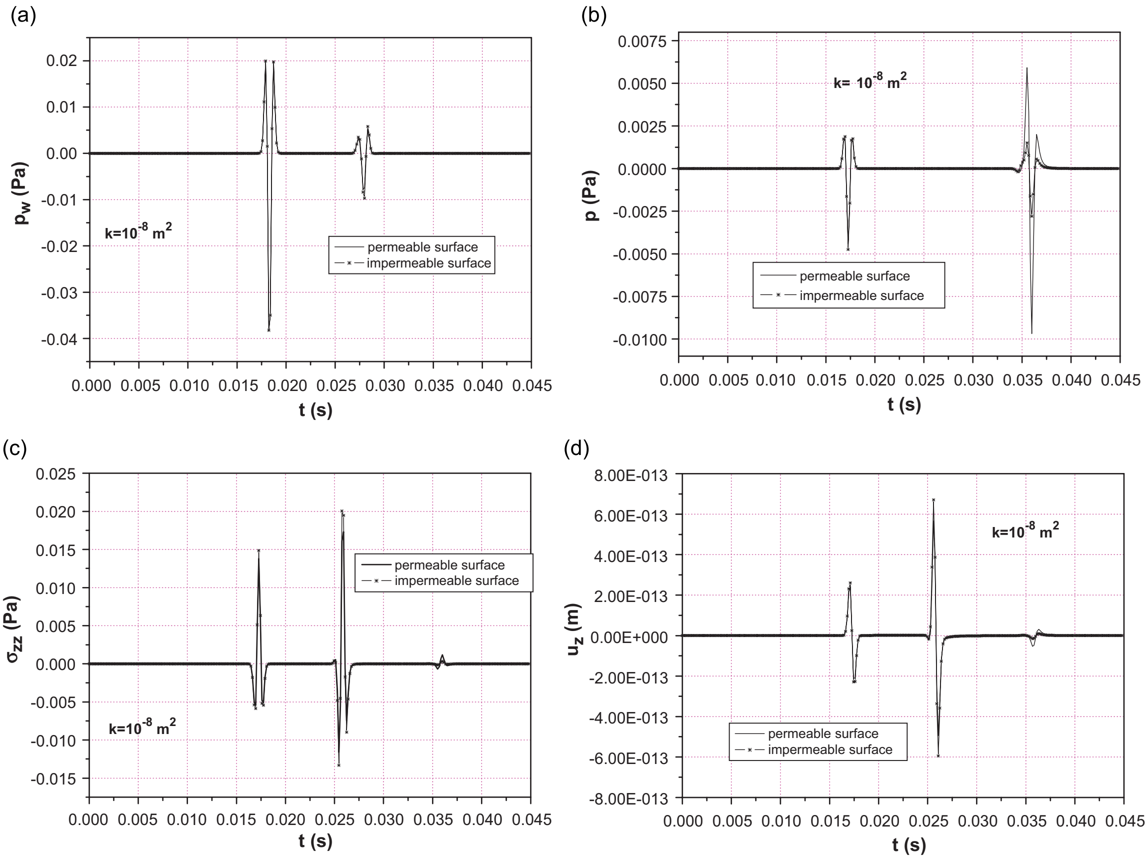

Fig. 4. The time domain response of the seawater and the seabed to an acoustic source located at $(r, z) = (0.0\,m, -10.0\,m)$ with the time history given by the Ricker wavelet function. The permeability of the seabed is equal to $k = 1.0 \times 10^{-8}$ and two cases for the seabed with a permeable and an impermeable surface are calculated: (a) the pressure p_w of the seawater at the point $(r, z) = (20\,m, -20\,m)$ for permeability $k = 1.0 \times 10^{-8}\,\mathrm{m^2}$; (b) the pore pressure p of the seabed at the point $(r, z) = (20\,m, 20\,m)$ for permeability $k = 1.0–10^{-8}\,\mathrm{m^2}$; (c) the stress σ_{zz} of the seabed at the point $(r, z) = (20\,m, 20\,m)$ for permeability $k = 1.0 \times 10^{-8}\,\mathrm{m^2}$; (d) the displacement u_z of the seabed at the point $(r, z) = (20\,m, 20\,m)$ for permeability $k = 1.0 \times 10^{-8}\,\mathrm{m^2}$.

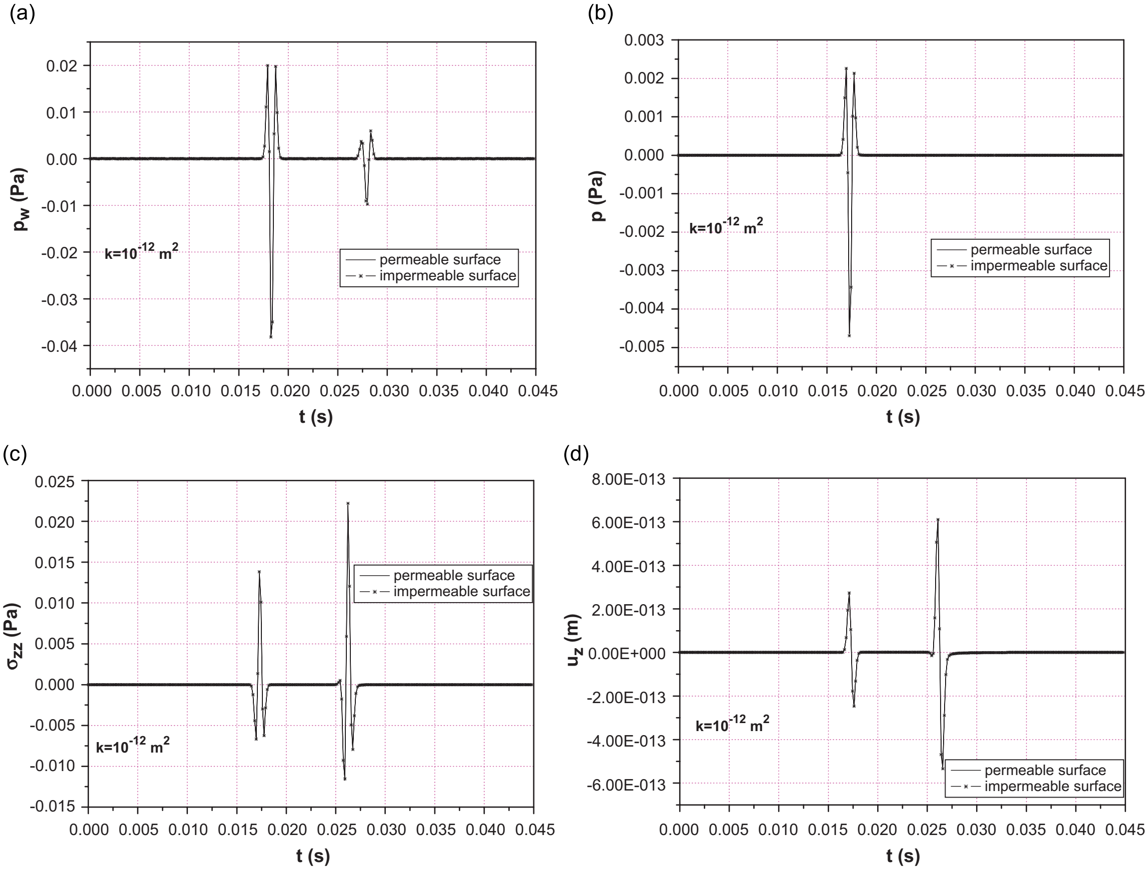

Fig. 5. The time domain response of the seawater and the seabed to an acoustic source located at $(r, z) = (0.0\,m, -10.0\,m)$ with the time history given by the Ricker wavelet function. The permeability of the seabed is equal to $k = 1.0 \times 10^{-12}\,\mathrm{m}^2$ and two cases for the seabed with a permeable and an impermeable surface are calculated: (a) the pressure p_w of the seawater at the point $(r, z) = (20\,m, -20\,m)$ for permeability $k = 1.0 \times 10^{-12}\,\mathrm{m}^2$; (b) the pore pressure p of the seabed at the point $(r, z) = (20\,m, 20\,m)$ for permeability $k = 1.0 \times 10^{-12}\,\mathrm{m}^2$; (c) the stress σ_{zz} of the seabed at the point $(r, z) = (20\,m, 20\,m)$ for permeability $k = 1.0 \times 10^{-12}\,\mathrm{m}^2$; (d) the displacement u_z of the seabed at the point $(r, z) = (20\,m, 20\,m)$ for permeability $k = 1.0 \times 10^{-12}\,\mathrm{m}^2$.

the FFT approach, the number of the sample points is $N = 281$; the sample spacing in the time domain is $\Delta t = 1.6 \times 10^{-4}\,\mathrm{s}$ and the sample spacing in the frequency domain is given by $\Delta\omega = 2\pi/(N\Delta t)\,\mathrm{s}^{-1}$.

Fig. 4(a) shows that two kinds of waves contribute to the pressure of the seawater: one is the direct incident wave due to the source; the other is the reflected wave from the surface of the seabed. As part of the energy of the wave incident on the seabed surface is transmitted into the seabed, the pressure of the seawater due to the direct incident wave is much larger than that due to the wave which is reflected from the surface of the seabed. Moreover, the continuity condition at the seabed surface (permeable or impermeable) almost makes no difference to the pressure of the seawater. For the seabed, again, we see that the continuity condition of the seabed has almost no influence on the pore pressure due to the P_1 wave. However, for the P_2 wave, the continuity condition has a significant influence on the pore pressure: the pore pressure of the permeable case is much larger than that of the impermeable case, which is obviously due to the fact that an impermeable seabed surface tends to prevent the relative motion between the pore fluid and the solid skeleton. Also, the shear wave of the porous medium has no contribution to the pore pressure of the seabed, which agrees with the constitutive relation of the pore fluid (Equation (14)). Fig. 4(c) and (d) indicate that all the three wave modes (the P_1, P_2, and the shear wave) of the porous medium contribute to the stress σ_{zz} and the displacement u_z. However, compared with the P_1 wave and the shear wave, the contribution from the P_2 wave is the smallest. Moreover, it follows from Fig. 4(c) and (d) that the continuity condition at the seabed surface has the largest influence on the P_2 wave; the second largest on the shear wave and the least on the P_1 wave. Fig. 5 illustrates that for the case $k = 1.0 \times 10^{-12}\,\mathrm{m}^2$, the P_2 wave is fully attenuated within the region near the seabed surface and thus, its influence on the response of the porous medium is invisible. Also, for $k = 1.0 \times 10^{-12}\,\mathrm{m}^2$, the high attenuation of the porous medium makes the relative motion between the pore fluid and the solid skeleton difficult, which make the difference between a permeable and an impermeable seabed surface negligible. Thus, the responses of the porous medium corresponding to the permeable case and the impermeable case are very close to each other (Fig. 5).

4. Conclusions

The closed-form Green's function in the frequency–wavenumber domain for an acoustic source in half-space seawater overlying a porous seabed has been established. The obtained Green's function is crucial for the BEM analysis of a seawater region near a porous seabed. The frequency domain Green's function for the seawater is separated into two parts: a singular part and a regular part. The singular part is in closed-form in the frequency domain, while the regular part can only be obtained by performing numerical inversion of the Hankel transform. By inversion of the Hankel transform, numerical results of Green's function in the frequency domain are obtained. Numerical results show that the permeability of the porous seabed has a very little influence on the response of the seawater, while the modulus M has an obvious influence on both the response of the seawater and the seabed. Based on the inverse Fourier transform method and the frequency domain Green's function, an example demonstrating the time domain response of the seawater and the seabed has also been presented.

Acknowledgments

This project is supported by the National Natural Science Foundation of China through Grant No. 50578071. The first author would also like to acknowledge the financial support received from the Chinese Education Department for returned overseas scholars. The authors are grateful for the special help from Miss Sally Williams for proofreading. Moreover, many constructive comments from the two anonymous reviewers are greatly appreciated.

References

[1] L.M. Brekhovskikh, Y.P. Lysanov, *Fundamentals of Ocean Acoustics*, Springer, New York, 1991.
[2] F.B. Jensen, W.A. Kuperman, M.B. Portor, H. Schmidt, *Computational Ocean Acoustics*, Springer, New York, 1997.
[3] S. Ahmad, P.K. Banerjee, Multi-domain BEM for two-dimensional problems of elastodynamics, *International Journal for Numerical Methods in Engineering* 26 (1988) 891–911.
[4] W.F. Florez, H. Power, F.C. Janna, Multi-domain dual reciprocity for the solution of inelastic non-Newtonian flow problems at low Reynolds number, *Computational Mechanics* 27 (2001) 396–411.
[5] R.D. Stoll, T.K. Kan, Reflection of acoustic waves at a water-sediment interface, *Journal of the Acoustical Society of America* 70 (1981) 149–156.
[6] K. Wu, Q. Xue, L. Adler, Reflection and transmission of elastic waves from a fluid-saturated porous solid boundary, *Journal of the Acoustical Society of America* 87 (1990) 2349–2358.
[7] A.I.M. Denneman, G.G. Drijkoningen, D.M.J. Smeulders, K. Wapenaar, Reflection and transmission of waves at a fluid/porous-medium interface, *Geophysics* 67 (2002) 282–291.
[8] S. Feng, D.L. Johnson, High-frequency acoustic properties of a fluid porous/solid interface. 1. New surface-mode, *Journal of the Acoustical Society of America* 74 (1983) 906–914.
[9] A.A. Gubaidullin, O.Y. Boldyreva, Wave propagation along the boundary between a saturated porous medium and a liquid, *Acoustical Physics* 52 (2006) 163–172.
[10] B. Albers, K. Wilmanski, Monochromatic surface waves on impermeable boundaries in two-component poro-elastic media, *Continuum Mechanics and Thermodynamics* 17 (2005) 269–285.
[11] B. Albers, Monochromatic surface waves at the interface between poroelastic and fluid half spaces, *Proceedings of the Royal Society A—Mathematical Physical and Engineering Sciences* 462 (2067) (2006) 701–723.
[12] S. Feng, D.L. Johnson, High-frequency acoustic properties of a fluid/porous solid interface. 2. The 2D reflection Green's function,, *Journal of the Acoustical Society of America* 74 (1983) 915–923.
[13] M.A. Biot, General theory of three-dimensional consolidation, *Journal of Applied Physics* 12 (1941) 155–164.

[14] M.A. Biot, Theory of propagation of elastic waves in a fluid-saturated porous solid, I, low frequency range, *Journal of the Acoustical Society of America* 28 (1956) 168–178.
[15] M.A. Biot, Theory of propagation of elastic waves in a fluid-saturated porous solid, II: higher frequency range, *Journal of the Acoustical Society of America* 28 (1956) 179–191.
[16] M.A. Biot, Mechanics of deformation and acoustic propagation in porous media, *Journal of Applied Physics* 33 (1962) 1482–1498.
[17] I.N. Sneddon, *Fourier Transforms*, McGraw-Hill, New York, NY, 1951.
[18] K. Aki, P.G. Richards, Quantitative Seismology: Theory and Methods, San Francisco, 1980.
[19] M. Abramowitz, I.A. Stegun, Handbook of Mathematical Functions with Formulas, Graphs, and Mathematical Tables, 10th ed., National Bureau of Standards Applied Mathematics Series, 1972, pp. 355–495.
[20] D.L. Johnson, J. Koplik, R. Dashen, Theory of dynamic permeability and tortuosity in fluid-saturated porous-media, *Journal of Fluid Mechanics* 176 (1987) 379–402.
[21] S.R. Pride, F.D. Morgan, A.F. Gangi, Drag forces of porous-medium acoustics, *Physical Review B* 47 (1993) 4964–4978.
[22] G. Bonnet, Basic singular solutions for a poroelastic medium in the dynamic range, *Journal of the Acoustical Society of America* 82 (1987) 1758–1762.
[23] A.N. Norris, Radiation from a point source and scattering theory in a fluid-saturated porous medium, *Journal of the Acoustical Society of America* 77 (1985) 2012–2023.
[24] C. Zimmerman, M. Stern, Scattering of plane compressional waves by spherical inclusions in a poroelastic medium, *Journal of the Acoustical Society of America* 94 (1993) 527–536.
[25] J.F. Lu, D.S. Jeng, A half-space saturated poro-elastic medium subjected to a moving load, *International Journal of Solids and Structures* 44 (2007) 573–586.
[26] P.M. Morse, H. Feshbach, *Method of Theoretical Physics, Part 1 and 2*, McGraw-Hill, New York, 1953, pp. 1759–1767.
[27] J.A. Ferrari, D. Perciante, A. Dubra, Fast Hankel transform of *n*th order, *Journal of the Optical Society of America A* 16 (1999) 2581–2582.
[28] E.W. Hansen, Fast Hankel transform algorithm, *IEEE Transactions on Acoustics Speech and Signal Processing* 33 (1985) 666–671.
[29] N.H. Ricker, *Transient Waves in Visco-elastic Media*, Elsevier, Amsterdam, 1977.